

# FT-IR Studies on Light Olefin Skeletal Isomerization Catalysis

## II. The Interaction of C4 Olefins and Alcohols with HZSM5 Zeolite

Marcella Trombetta,\* Guido Busca,\* Stefano Rossini,† Valerio Piccoli,† and Ugo Cornaro†

\* *Istituto di Chimica, Facoltà di Ingegneria, Università di Genova, P.le J.F. Kennedy, I-16129 Genoa, Italy; and* † *Snamprogetti, via Maritano 26, I-20097 San Donato Milanese, Milan, Italy*

Received July 15, 1996; revised November 4, 1996; accepted January 24, 1997

The catalytic activity of the zeolite HZSM5 in *n*-butene conversion was investigated under conditions similar to those of a commercial process for skeletal isomerization. The catalyst was found to be very active in *n*-butene conversion, but selectivity to isobutene was low due to a predominance of cracking, coking, and oligomerization side reactions. The interaction of 1-butene, *cis*-2-butene, *trans*-2-butene, isobutene, *sec*-butanol, and *tert*-butanol was also investigated by FT-IR spectroscopy in the temperature range 150–673 K. *n*-Butenes were first adsorbed on the acidic OHs of the zeolite giving rise to well-defined hydrogen-bonded species. These species probably undergo protonation to the corresponding carbenium ion, which could, however, not be detected, and later, through skeletal isomerization/alkylation/skeletal isomerization sequences, to polyisobutene. In the case of isobutene, a *tert*-butoxy species supposed to act as the precursor for *tert*-butyl carbenium ions, active as the cationic polymerization initiator, was detected and characterized spectroscopically. Starting from isobutene, the polymerization is partly hindered at low temperature because of the limited diffusion of the olefin into the zeolite pores. The alcohols dehydrate around room temperature and also give rise to polyisobutene in the same way. © 1997 Academic Press

### INTRODUCTION

The skeletal isomerizations of *n*-butene to isobutene and of *n*-pentene to isoamylene are topics of increasing interest (1) because of the increased demand for isoolefins, in relation to the demand for branched ethers (MTBE, ETBE, and TAME) for reformulated gasoline (2). Very recently, the use of different protonic zeolites was proposed for these reactions (3–7). In particular, ferrierite (3, 6) was reported to be a very promising catalytic material for the conversion of *n*-butene to isobutene. ZSM5 zeolite is also active for this reaction, although selectivity is quite low (1, 8, 9) due to the concurrence of oligomerization, transmutation, disproportionation, and aromatization reactions.

This reaction is certainly catalyzed by protonic acids (10–12). It is believed that the normal olefins undergo an electrophilic attack from the proton to produce a secondary

carbenium ion that later transposes to a more stable tertiary carbenium ion (10–12), the precursors for branched olefins. The formation of protonated alkylcyclopropane intermediates was proposed several years ago (13). However, in the case of the C4 carbenium ion skeletal isomerization, a difficulty arises. In fact, the simple opening of the protonated methylcyclopropane ring implies the intermediate formation of a very unstable primary isobutyl carbenium ion. This can be avoided either if the ring opening occurs, in a concerted way, directly to the *tert*-butyl cation (13) or if a previous dimerization (3) gives rise to a C8 carbenium ion that can more easily isomerize and crack back to isobutene (14). This mechanistic problem can be related to the reason why ferrierite is more selective than other zeolites, like ZSM5, in *n*-butene skeletal isomerization. In fact the channels of ferrierite are slightly smaller in size than those of ZSM5 and this suggested two nearly opposing interpretations. Mooiweer *et al.* (3) proposed that the dimensions of the cavities in ferrierite catalysts would fit the size of the C8 dimers, allowing their formation, their capture, and their cracking back to isobutene before their desorption. On the contrary, Millini and Rossini (9) proposed that the ferrierite cavities are too small to allow dimerization, thus favoring selective skeletal isomerization to occur with a “monomolecular” mechanism.

We approached these problems using IR spectroscopy and flow reactor experiments over different catalytic materials (15, 16). We present here the data of the study of the interaction of the C4 olefins with the protonic zeolite HZSM5.

### EXPERIMENTAL

A commercial HZSM5 catalyst (Si/Al atomic ratio = 23) (Engelhard) was used. The IR spectra were recorded on a Nicolet Magna 750 Fourier transform instrument, using pressed disks of pure zeolite powder, activated by outgassing at 773 K into the IR cell.

The catalytic tests reported here were performed with 0.8 atm 1-butene (81.04 kPa, dilution with isobutane) under

the conditions reported in Table 1 with a fixed-bed tubular reactor (internal diameter 12 mm, with a coaxial internal thermocouple with 5 mm external diameter). The catalyst granulometry was 20–25 mesh. The products were recovered integrally for either 20 or 40 min on stream and were analyzed by on-line gas chromatography (HP 5890) using a FID detector and a 50-m Chrompack PLOT Al<sub>2</sub>O<sub>3</sub>/Na<sub>2</sub>SO<sub>4</sub> capillary column for 1-butene/isobutene separation and a 50-m PONA capillary column for the analysis of all other products.

## RESULTS

### (a) Catalytic Activity

The catalytic activity of the zeolite ZSM5, measured under conditions similar to those of an industrial process with catalysts based on aluminas (15–17), is given in Table 1. The results of three typical experiments are reported. It is evident that, under these conditions, the catalyst is very active in the conversion of *n*-butene, much more than alumina and silicated aluminas (16, 17). Skeletal isomerization to isobutene occurs, and the isobutene to total butenes concentration ratio ( $\approx 0.43$ ), obtained in all three cases, even exceeds slightly the equilibrium value measured by Kilpatrick *et al.* (18), showing that some of the isobutene probably arises from cracking of higher hydrocarbons such as the C<sub>8</sub> dimeric species (3).

However, the selectivity to the desired product, isobutene, is strongly affected by unwanted side reactions, which can be broadly classified as dimerization/cracking to C<sub>5</sub> + C<sub>3</sub> hydrocarbons, hydrogenation to C<sub>4</sub> paraffins, and aromatization. Hydrogen arising from aromatization and coking may be responsible for hydrogenation to butanes. These data are in more or less agreement with those reported recently for the same catalytic system (1, 3, 9) and which showed that, even at lower conversions, the selectivity to isobutene on ZSM5 does not exceed 15%.

### (b) Interaction of 1-Butene with the HZSM5 Surface

Figure 1a gives the IR spectrum of the surface hydroxy groups on our ZSM5 sample, recorded at 300 K, after previous activation at 773 K. The spectrum agrees with those reported previously for the same catalyst (19–21). It shows

a weak sharp maximum at 3747 cm<sup>-1</sup>, with a shoulder at lower frequency (3730 cm<sup>-1</sup>), a broad band with components at 3690 and 3677 cm<sup>-1</sup>, and, finally, a very intense band at 3612 cm<sup>-1</sup>. All bands shift slightly toward higher frequencies by cooling down to 170 K (see low-temperature experiments, below) when the stronger band is observed at 3623 cm<sup>-1</sup>. According to the literature, the stronger band is associated with the strongly Brønsted acidic OHs of the ZSM5 zeolite, while the broad band in the region 3700–3650 cm<sup>-1</sup> is due to the OHs of extraframework alumina. Finally, the weak band at 3747 cm<sup>-1</sup> is due to nonacidic silanol groups related to Al-free silicalite-type grains, exposed at the external surface. The weak component at 3730 cm<sup>-1</sup> is likely associated with nonacidic silanols located in internal pores like those of silicalite (21, 22). These data and the relative intensity of the above  $\nu$ OH bands characterize our sample as a typical ZSM5 zeolite with high Al content and with significant amounts of extraframework alumina.

The contact of the activated ZSM5 sample with 1-butene gas at room temperature (Fig. 1b) gives rise to the immediate disappearance of the strong  $\nu$ OH band of the acidic OHs at 3612 cm<sup>-1</sup>, while the other  $\nu$ OH bands appear to be almost unperturbed. This perturbation resists outgassing at room temperature. The IR spectra of the surface species, resulting from the interaction of 1-butene with the ZSM5 surface, are also shown in the CH stretching and CH deformation regions in Fig. 1, middle and right panels. It is evident that a hydrocarbon species, stable under outgassing at room temperature, is formed. In fact, outgassing causes only the partial disappearance of a weak shoulder at 3020 cm<sup>-1</sup>, which is a typical position of the asymmetric CH stretching of 1,2-disubstituted ethylenes such as 2-butenes or higher “internal” olefins. The main absorptions in the spectrum are unaffected by outgassing at room temperature. They are observed at 2960, 2936, 2870 (shoulder), and 2860 cm<sup>-1</sup> (saturated C–H stretchings), at 1470, 1457, and 1441 cm<sup>-1</sup> (asymmetric CH<sub>3</sub> deformations and CH<sub>2</sub> scissoring), and at 1381 (stronger) and 1370 cm<sup>-1</sup> (weaker, CH<sub>3</sub> symmetric deformation). The spectrum of this species, where no bands assignable to =C–H stretchings (3100–3000 cm<sup>-1</sup>) or to C=C stretchings (1680–1600 cm<sup>-1</sup>) of olefinic species are detectable, is certainly due neither to butene isomers nor to higher olefins. On the contrary, the spectrum is typical of saturated hydrocarbon species,

TABLE 1

*n*-Butene Conversion Data on ZSM5 Zeolite (Three Different Experiments)

<i>W</i> <sub>cat</sub> (g)	LHSV (h <sup>-1</sup> )	<i>T</i> (K)	<i>P</i> (atm)	<i>T</i> <sub>1</sub> <sup>a</sup> (min)	<i>T</i> <sub>2</sub> <sup>a</sup> (min)	Conv. (%)	<i>S</i> <sub>iso</sub> (%)	<i>S</i> <sub>C1-C3</sub> (%)	<i>S</i> <sub>C3=</sub> (%)	<i>S</i> <sub>C4sat</sub> (%)	<i>S</i> <sub>C5</sub> (%)	<i>S</i> <sub>arom</sub> (%)
0.6	20.27	733	0.8	20	40	87.80	10.44	24.41	18.28	11.59	17.75	3.59
0.6	23.65	723	0.8	20	40	84.54	13.07	16.39	13.65	8.35	23.18	2.74
0.6	27.34	723	0.8	220	260	84.30	13.60	20.74	16.87	6.50	23.06	2.07

<sup>a</sup> *T*<sub>1</sub> and *T*<sub>2</sub> are the respective times on stream of starting and stopping product collection.

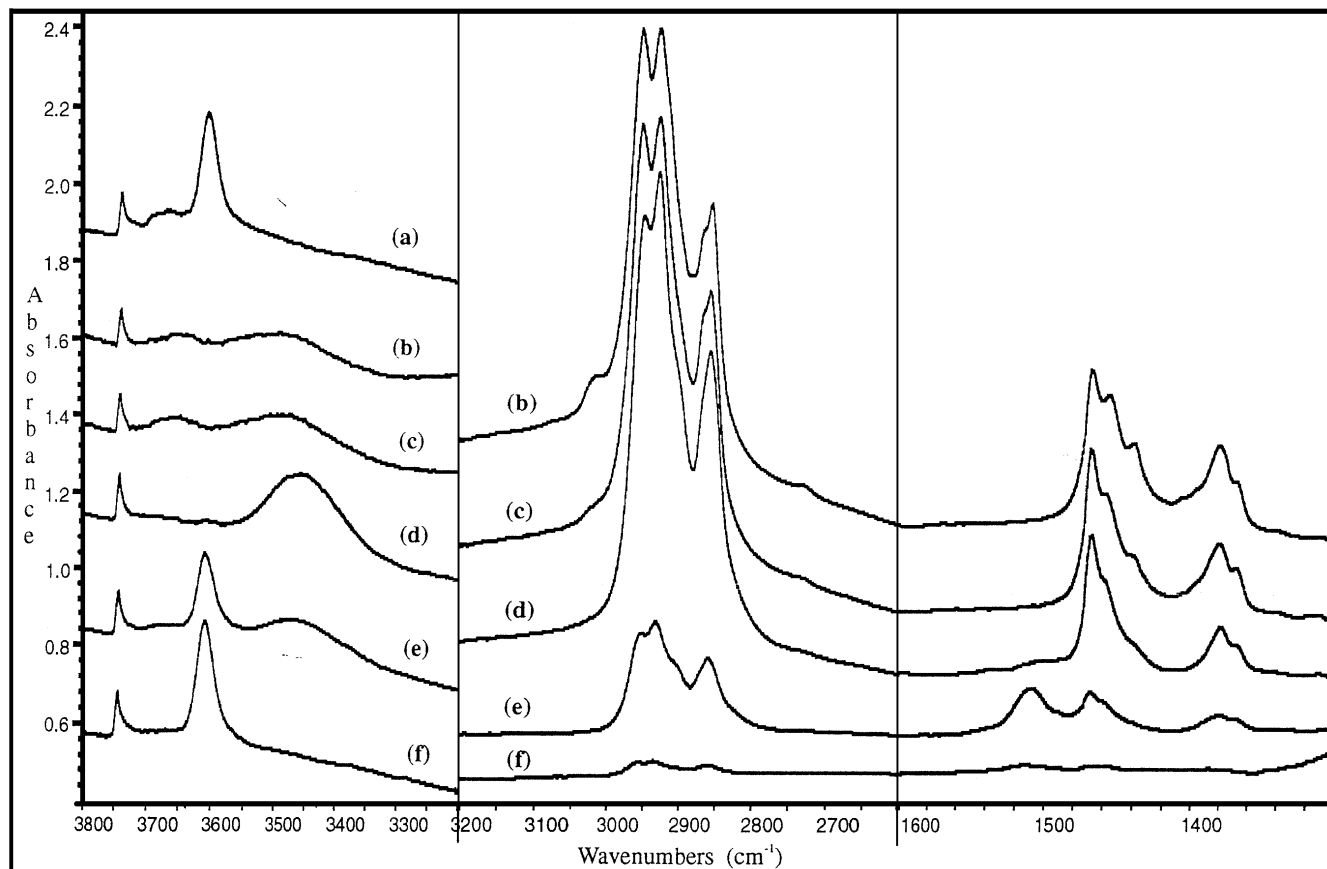


FIG. 1. FT-IR spectra of the HZSM5 catalyst in the OH stretching region (left) and of the adsorbed species (middle, right) before (a) and after adsorption of 1-butene at 300 K in contact with the gas (b) and after outgassing at 300 K (c), 373 K (d), 473 K (e), and 573 K (f); all spectra were recorded at 300 K.

thus being very likely due to a polymeric species. The clear splitting of the symmetric  $\text{CH}_3$  deformation mode at 1383 and  $1368\text{ cm}^{-1}$ , with the higher-frequency band significantly stronger than the lower-frequency one, provides evidence of the predominance of isopropylidene  $\text{C}-\text{C}(\text{CH}_3)_2-\text{C}$  fragments (i.e., geminal methyls) (23). The overall spectrum has many details in contrast with that of poly-1-butene (24), while it seems to be fully consistent with that of polyisobutene (25–27).

This polymeric species is fully stable at 373 K but disappears partially as a result of outgassing at 473 K and completely at 573 K (Figs. 1e and 1f). In parallel, the  $\nu\text{OH}$  band of the acidic OHs at  $3612\text{ cm}^{-1}$  is completely restored only at 573 K. This is likely due to the depolymerization reaction. However, we must note that, after outgassing at 473 K, an additional rather strong band is detected at  $1520\text{ cm}^{-1}$  (Fig. 1e), together with the residual bands of the polymer. This band must be assigned to a transformation product of the polymer. A band in the range  $1530\text{--}1480\text{ cm}^{-1}$  was detected by several researchers after heating olefins over protonic zeolites such as HZSM5; their possible assignments were discussed recently by Demidov and Davydov (28). It was assigned, by other researchers, to aromatic species

(ring  $\text{C}=\text{C}$  stretching), to carboxylate species (asymmetric  $\text{COO}$  stretching), to “nonclassical” carbenium ions, or, finally, to allyl cations ( $\text{C}=\text{C}$  stretching). The last assignment, supported by the work of Demidov and Davydov (28), is mostly based on the simultaneous detection of characteristic UV-visible absorptions. We are not yet able to give additional information on the nature of this species.

The contact of the activated ZSM5 sample with 1-butene gas at 170 K (Fig. 2) also gives rise to the immediate disappearance of the  $3620\text{ cm}^{-1}$  band. However, under these conditions, an extremely broad absorption is formed, centered near  $3000\text{ cm}^{-1}$ . Superimposed over this absorption, the  $\text{C}-\text{H}$  stretching bands of a hydrocarbon species can be also found. At the same time,  $\text{CH}$  deformation bands were found in the region  $1600\text{--}1300\text{ cm}^{-1}$  (Fig. 3). The spectrum observed under these conditions is that of the olefin, weakly perturbed. The position of the bands recorded under these conditions was reported in the first paper of this series (Table 2 in Ref. (16)). In particular, the  $=\text{CH}_2$  asymmetric stretching mode observed at  $3079\text{ cm}^{-1}$ , the first overtone of the  $=\text{CH}_2$  wagging mode observed split at 1823 and  $1861\text{ cm}^{-1}$ , and the  $\text{C}=\text{C}$  double-bond stretching observed split at 1641 and  $1628\text{ cm}^{-1}$  provide evidence that

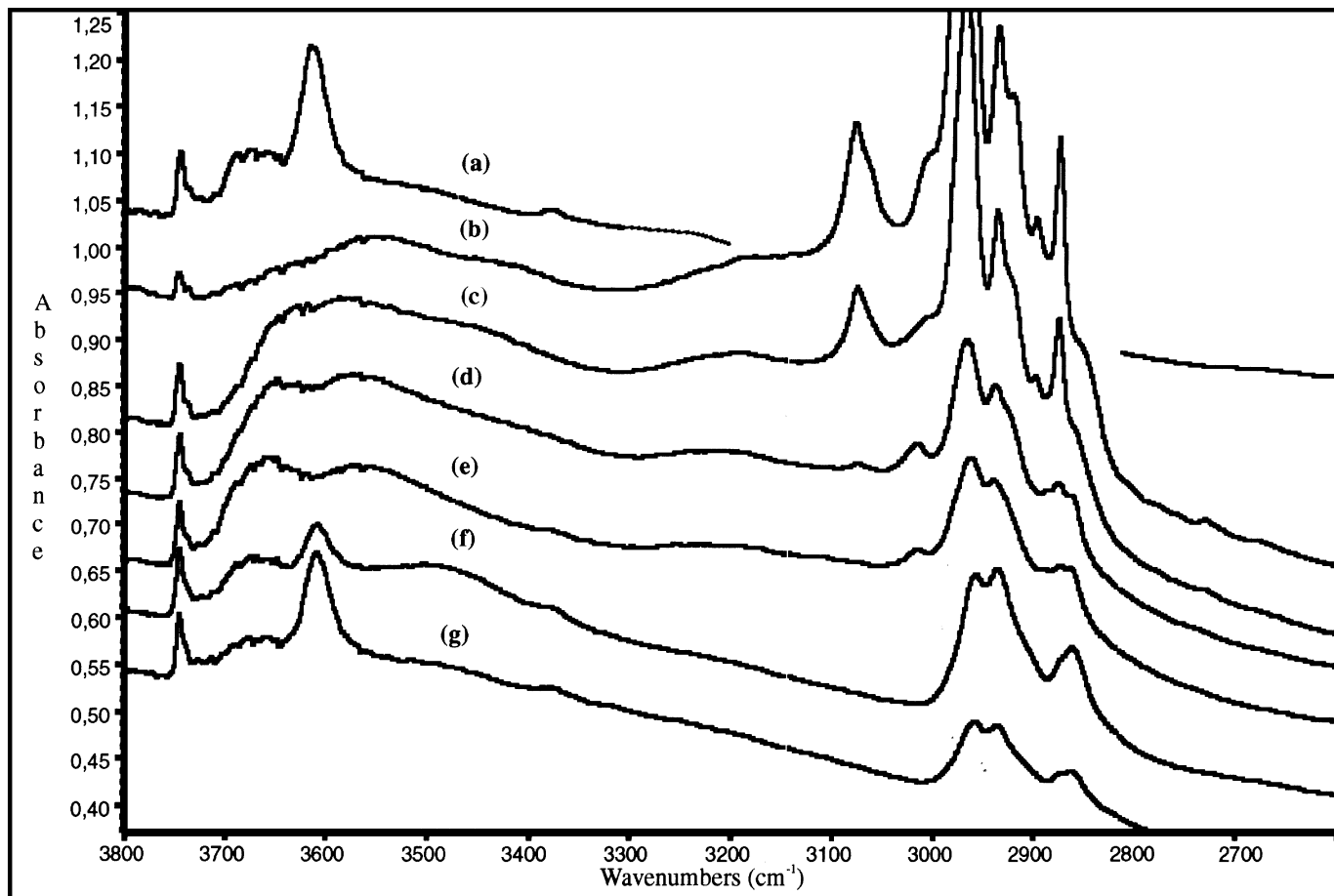


FIG. 2. FT-IR spectra ( $3800\text{--}2600\text{ cm}^{-1}$ ) of the HZSM5 catalyst in the OH/CH stretching region, after outgassing at 773 K and cooling down to 170 K (a), after contact with 1-butene gas at 170 K (b) and after successive outgassing at 210 K (c), 240 K (d), 260 K (e), 323 K (f), and 373 K (g).

the olefin is adsorbed intact in two different forms. The position of these modes is shifted with respect to the gas phase molecule ( $3089\text{ cm}^{-1}$ ,  $\nu_{\text{as}}\text{CH}_2$ ;  $1833\text{ cm}^{-1}$ , the overtone of  $w\text{CH}_2$ ;  $1644$ ,  $1648\text{ cm}^{-1}$ ,  $\nu\text{C}=\text{C}$  of the two conformers, *s-cis* and *gauche*), showing that the molecule undergoes a weak electron withdrawal on its  $\text{C}=\text{C}$  double bond. These features strongly support the conclusion that, at 170 K, some of the 1-butene molecules interact via an H-bonding on its  $\pi$  orbital with the acidic OHs of the zeolite ( $\nu\text{C}=\text{C}$  at  $1628\text{ cm}^{-1}$ ;  $2w\text{CH}_2$  at  $1861\text{ cm}^{-1}$ ), while part of it is simply liquefied into the ZSM5 zeolite cavities ( $\nu\text{C}=\text{C}$  at  $1641\text{ cm}^{-1}$ ;  $2w\text{CH}_2$  at  $1823\text{ cm}^{-1}$ ). The internal acidic OHs undergo a spectacular shift down to almost  $3000\text{ cm}^{-1}$  as well as broadening, while the nonacidic external silanols appear to be unperturbed.

This interpretation is supported when the temperature is raised. The bands at  $1641$  and  $1823\text{ cm}^{-1}$ , assigned to liquefied 1-butene, disappear completely when warmed in the range 170 to 230 K (according to its boiling point of 267 K at 1 atm = 101.3 kPa (29)), while those assigned above to H-bonded species resist outgassing in this temperature range.

Further warming in the range 230 to 270 K causes the complete modification of the spectrum. The bands due to molecularly adsorbed 1-butene disappear completely, and a spectrum very similar to that observed upon interaction at room temperature and assigned to polyisobutene becomes apparent, though weaker. In this temperature range, the  $\nu\text{OH}$  band of the free acidic OHs is not restored (Fig. 2e), but the broad band in the range near  $3000\text{ cm}^{-1}$  disappears.

Our experiments do not show any spectroscopic features of intermediate species between H-bonded 1-butene and adsorbed polyisobutene except for a band at  $3020\text{ cm}^{-1}$  observed upon interaction both at room temperature and at lower temperatures (220–270 K); this band is due neither to 1-butene nor to polyisobutene. A possible assignment of this band to the  $\text{C-H}$  stretching of an “internal” olefin, such as 2-butene, or of an oligomeric species is proposed.

#### (c) Interaction of *cis*- and *trans*-2-Butene with the HZSM5 Surface

The experiments on the interaction of both *cis*-2-butene and *trans*-2-butene with HZSM5 give rise to very similar

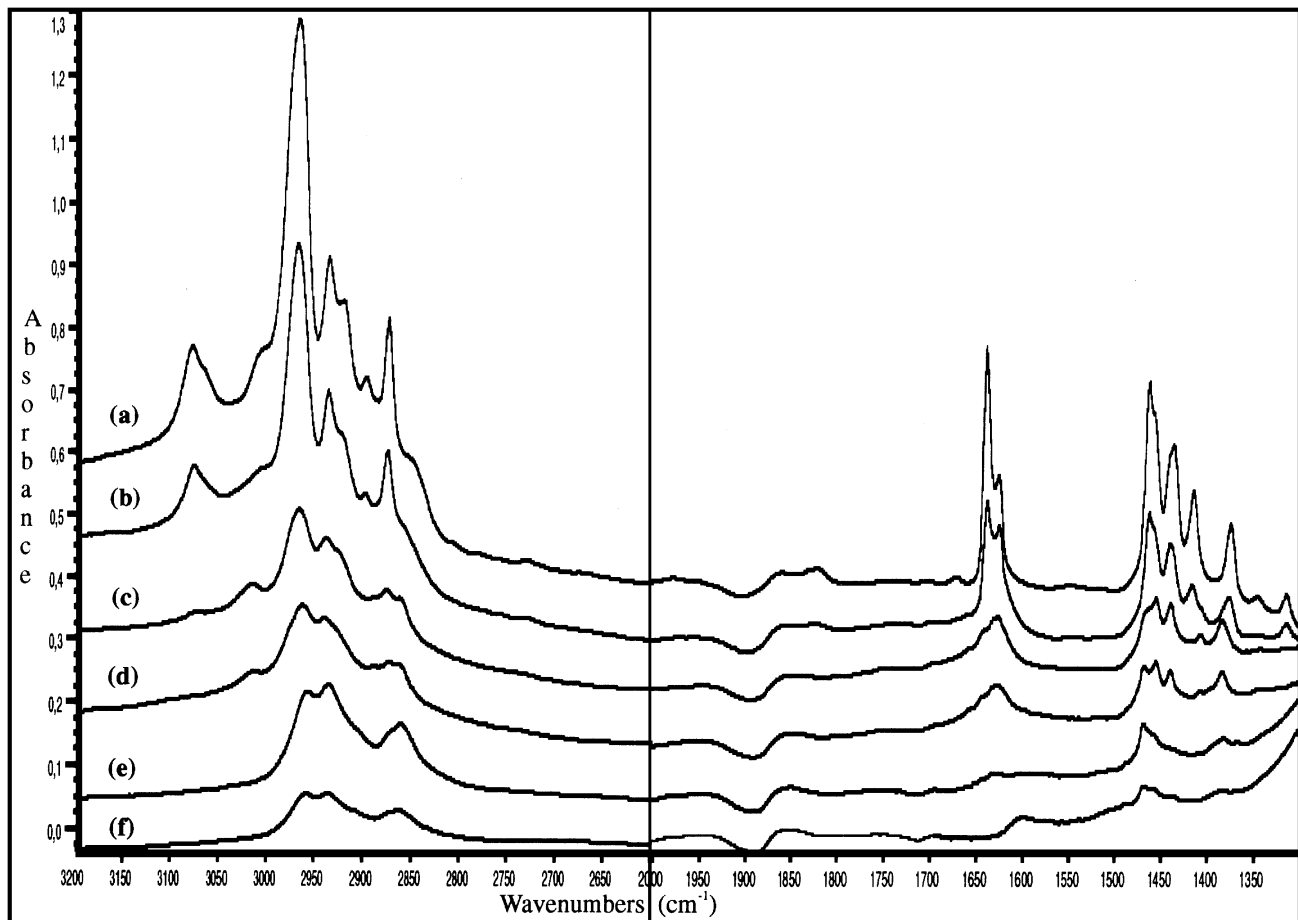


FIG. 3. FT-IR spectra of the adsorbed species arising from 1-butene adsorption on HZSM5 at 170 K (a) and after successive outgassing at 210 K (b), 240 K (c), 260 K (d), 323 K (e), and 373 K (f).

results with respect to those described above for 1-butene. In both cases of the adsorption of 2-butene geometric isomers on ZSM5 at room temperature (Figs. 4a and 4b for *cis*-2-butene; Figs. 4c and 4d for *trans*-2-butene), the spectra are dominated by the same spectrum, assigned above to polyisobutene. The spectra of the species arising from the three linear butene isomers are virtually identical. Under these conditions, the OH band at  $3615\text{ cm}^{-1}$  disappeared, while it reappeared after heating to around 473 K when the polymeric species is destroyed. The picture in the OH stretching region upon 2-butenes adsorption at room temperature is consistent with the above for 1-butene interaction at room temperature (Fig. 1).

Still in contact with 2-butene gases, weak bands were found at 1661, 1645, and  $1625\text{ cm}^{-1}$ . These correspond closely to the C=C stretchings of *trans*-2-butene, *cis*-2-butene, and 1-butene, respectively, adsorbed as such at low temperatures (see below). We suppose, therefore, that the double-bond isomerization and the *cis*-*trans* isomerization reactions occur already at room temperature over the strongly acidic OHs of ZSM5 zeolite.

At temperatures near 170 K, the interaction of the ZSM5 zeolite with the two 2-butenes (Fig. 5) shows the bands assigned to the molecular species. The splitting of the C=C stretching band of *cis*-2-butene at 1663 and  $1645\text{ cm}^{-1}$  is again due to the presence of liquefied *cis*-2-butene and of *cis*-2-butene interacting with the acidic hydroxy groups, whose band is again shifted from  $3623\text{ cm}^{-1}$  to near  $3000\text{ cm}^{-1}$ , and is very broad. In the case of the *trans*-2-butene isomer, the band of the liquid-like species was not detected, according to the centrosymmetry of the molecule that makes it IR inactive ( $1682\text{ cm}^{-1}$  in the Raman spectrum of the gas). A medium weak band at  $1657\text{ cm}^{-1}$  is instead associated with  $\nu\text{C}=\text{C}$  of the species interacting with the surface OHs, made IR active due to the asymmetry induced by the interaction.

A careful analysis of the spectra relative to the low-temperature adsorption of the three *n*-butene isomers shows that the liquid-like monomeric species always disappear in the range 240 to 270 K; the H-bonded species disappear in the range 260 to 290 K, while in the same range typical absorptions of the polymer form.

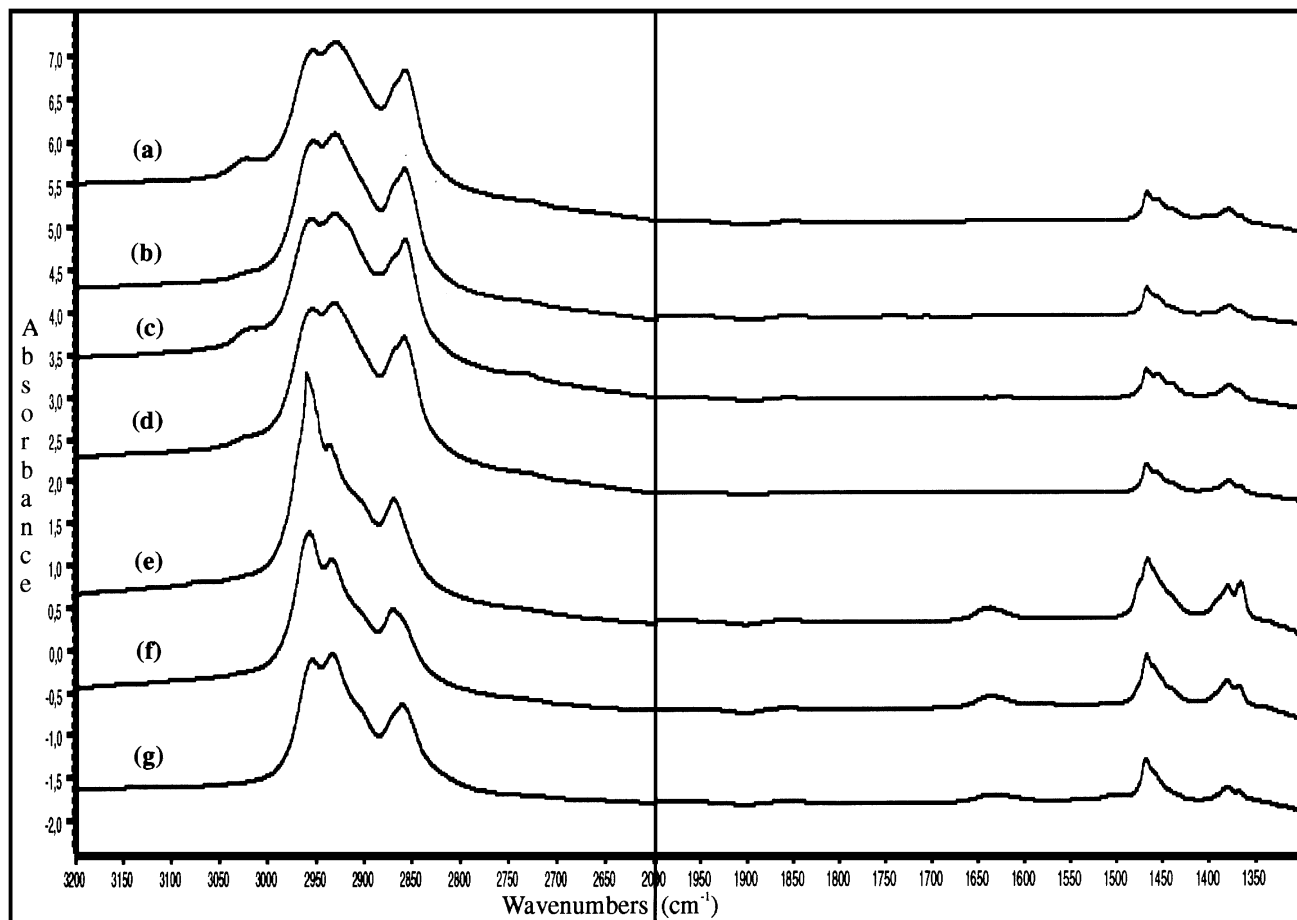


FIG. 4. FT-IR spectra of the adsorbed species arising from the adsorption of *cis*-2-butene (a, b), *trans*-2-butene (c, d), and isobutene (e, f, g) on HZSM5 at 300 K in contact with the gas (a, c, e) and after outgassing at 300 K (b, d, f) and 373 K (g).

#### (d) Interaction of Isobutene with the HZSM5 Surface

The interaction of the HZSM5 catalyst with isobutene at room temperature, followed by outgassing at room temperature (Figs. 4e and 4f), gives rise to spectra that are similar to those observed under the same conditions upon interaction with the three linear butenes. After treating at 373 K the spectra obtained from the four butene isomers were virtually identical. This fully supports our previous assignment of the observed spectra arising from *n*-butenes to polyisobutene. Based on the similarity of the spectra of the species formed from isobutene at room temperature (which is not the same recorder after treating at 373 K) with those of isobutene oligomers (27), it seems plausible to conclude that low oligomers of isobutene are formed first, while only at 373 K can they give rise to higher polymers. This may be an effect of limited diffusion of branched hydrocarbon species in the ZSM5 cavities. However, the interaction of isobutene at lower temperatures gives rise to an even more complex picture.

The experiment on the interaction of isobutene with HZSM5 at low temperature gives us a better understand-

ing of what happens (Fig. 6). The spectrum recorded upon interaction at 170 K again exhibits the features of isobutene interacting as such with the surface OHs ( $\nu\text{C}=\text{C}$  at  $1639\text{ cm}^{-1}$ ) and simply liquified ( $\nu\text{C}=\text{C}$  at  $1659\text{ cm}^{-1}$ ;  $2\nu\text{CH}_2$  at  $1780\text{ cm}^{-1}$ ), together with the features of another species. The adsorbed forms of isobutene disappear upon outgassing below 230 K, while the second species is not affected. The spectrum of this species does not correspond to that of the polymer formed by *n*-butenes at room temperature and by isobutene at 373 K, which we assigned to polyisobutene or to the polymeric species formed by isobutene at room temperature. It does not show any evident CH stretching above  $3000\text{ cm}^{-1}$ , thus showing that olefinic  $=\text{CH}_2$  or  $\text{H}-\text{C}=\text{C}-\text{H}$  groups are not present. This "intermediate" species, between the H-bonded monomer and the polymer, is characterized in the CH stretching region by a strong band near  $2985\text{ cm}^{-1}$ , i.e., at frequencies higher than the strongest  $\nu\text{CH}$ s of the polymer. At the lower-frequency side of this band, weaker absorptions, due either to small amounts of the polymer (already formed) or to the species itself, are also present. Under the same conditions, in the lower-frequency region the following features

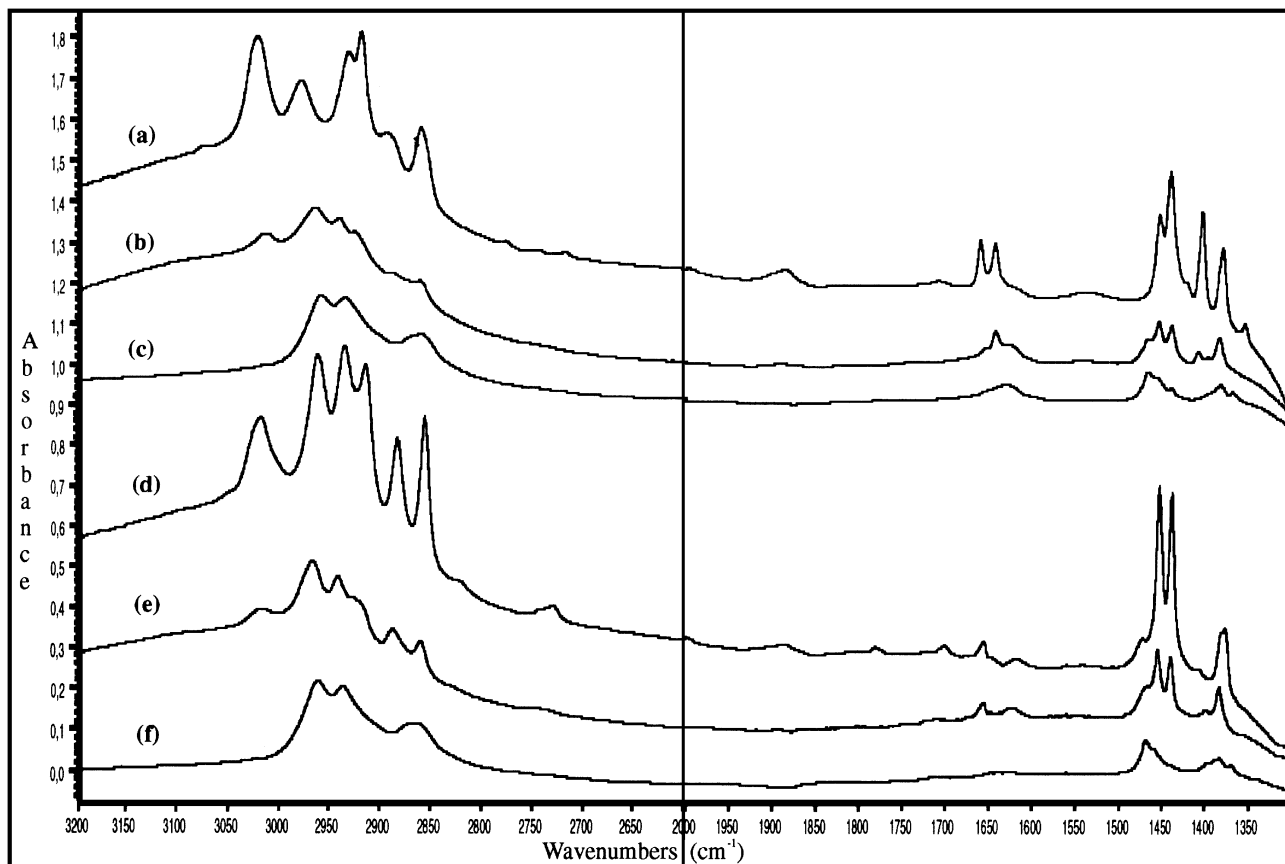


FIG. 5. FT-IR spectra of the adsorbed species arising from *cis*-2-butene (a, b, c) and *trans*-2-butene (d, e, f), adsorption on HZSM5 at 170 K (a, d) and after successive outgassing at 260 K (b, e) and 300 K (d, f).

were recorded:

(i) the complex band due to symmetric methyl deformations ( $1410\text{--}1350\text{ cm}^{-1}$ ) is more intense than that where the asymmetric methyl deformations fall ( $1500\text{--}1420\text{ cm}^{-1}$ );

(ii) in the asymmetric  $\text{CH}_3$  deformation region the strongest band is near  $1470\text{ cm}^{-1}$ , but a component at  $1480\text{ cm}^{-1}$  is clearly resolved; and

(iii) three peaks are observed in the  $\text{CH}_3$  symmetric deformation region, at  $1405$ ,  $1380$  (main maximum), and  $1370\text{ cm}^{-1}$ .

The bands at  $1480$  and  $1405\text{ cm}^{-1}$  behave in the same way as the band at  $2985\text{ cm}^{-1}$ , and could characterize the intermediate species.

To better define the nature of this intermediate species, we put a very small amount of isobutene gas ( $P < 0.1\text{ Torr}$ ;  $0.1\text{ Torr} = 13.3\text{ N m}^{-2}$ ) at  $250\text{ K}$  into contact with HZSM5. The resulting surface species are characterized by the spectrum in Fig. 7a. It seems that, in this spectrum, in spite of the very weak amount of olefin contacted, the features of the polymer (spectrum reported in Fig. 7b) are already present together with those of the so-called intermediate species. Thus, we could subtract them from the spectrum and ob-

tain the subtraction spectrum reported in Fig. 7c, which we assigned to the intermediate species. It is characterized by a sharp  $\nu_{\text{as}}\text{CH}_3$  band at  $2985\text{ cm}^{-1}$  with weak  $\nu\text{CH}$  components near  $2945$ ,  $2918$ , and  $2885\text{ cm}^{-1}$  and by a complex  $\delta_{\text{as}}\text{CH}_3$  band with a maximum at  $1480\text{ cm}^{-1}$  and a clear  $\delta_{\text{sym}}\text{CH}_3$  doublet at  $1405$  and  $1380\text{ cm}^{-1}$ , the former being clearly weaker than the latter. The last doublet is typical of *tert*-butyl groupings (23), and the overall spectrum seems to be consistent with those of *tert*-butoxy species, like those we previously characterized on  $\text{TiO}_2$  (30) and on  $\gamma\text{-Al}_2\text{O}_3$  (16). To confirm the possible identification of the intermediate species as a *tert*-butoxy-group, we investigated the interaction of *tert*-butanol with HZSM5 and with pure silica. As will be discussed below, *tert*-butanol on HZSM5 zeolite interacts primarily through its alcoholic OH group with the acidic OHs of the zeolite, giving rise to dehydration to isobutene. For this reason, we did not observe the details of the spectroscopic features of the surface alkoxides. Instead, on amorphous silica (Aerosil 130 from Degussa), the interaction at  $373\text{ K}$  gives rise to "etherification" of the surface OHs, allowing the detection of a good spectrum due to the  $(\text{CH}_3)_3\text{C-O-Si}$  surface species (Fig. 7d). The spectrum is virtually identical with respect to that observed at

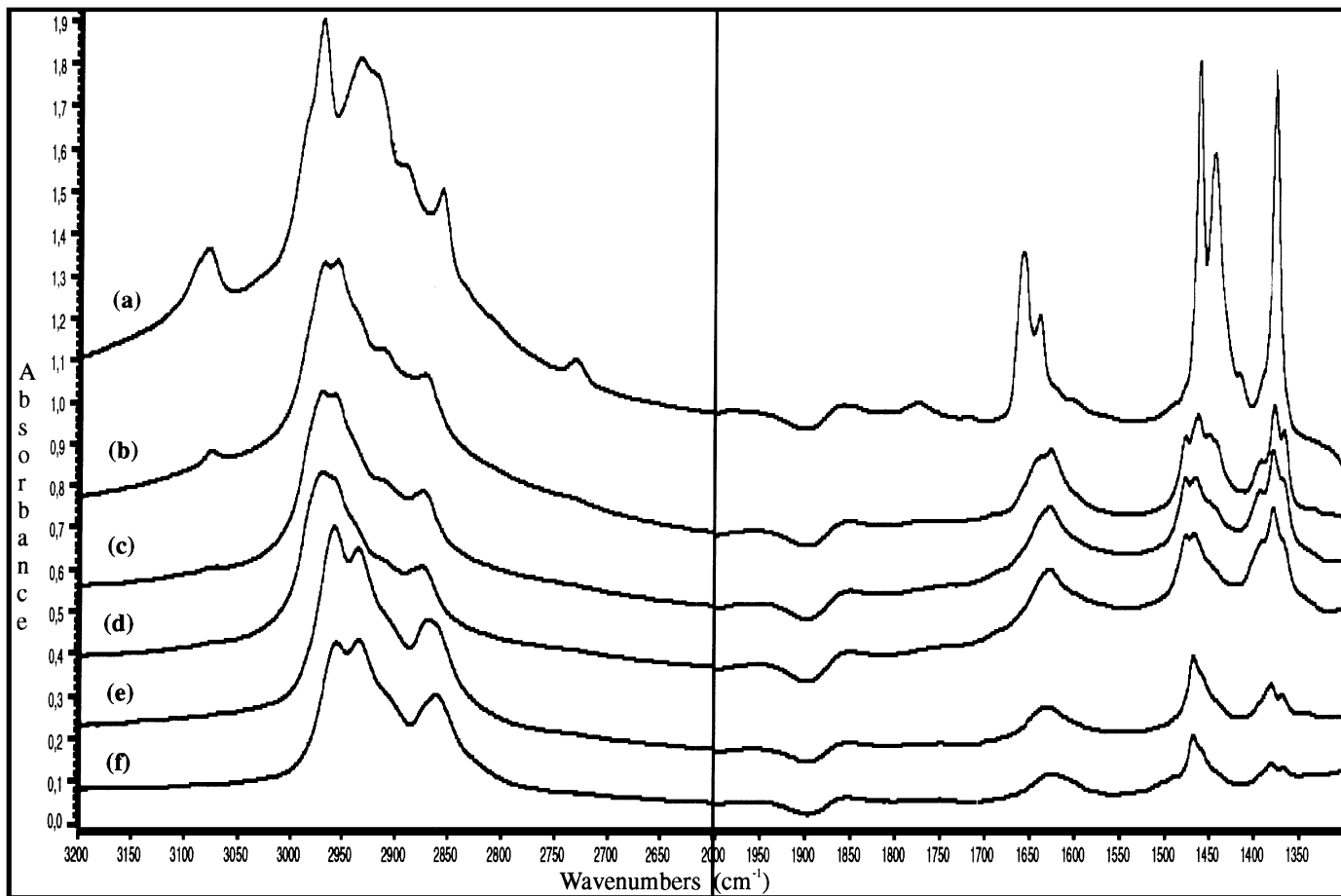
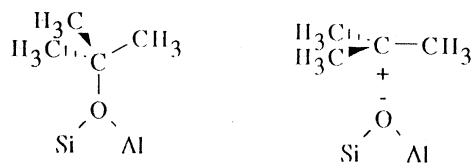


FIG. 6. FT-IR spectra of the adsorbed species arising from isobutene adsorption on HZSM5 at 170 K (a) and after successive outgassing at 210 K (b), 240 K (c), 260 K (d), 323 K (e), and 373 K (f).

low temperature for isobutene on HZSM5 and allows us to identify the intermediate species as a  $(\text{CH}_3)_3\text{C}-\text{O}-\text{Si}$  surface species (i.e., a *tert*-butoxy group).

Isobutene does not give rise to *tert*-butoxy groups on  $\gamma\text{-Al}_2\text{O}_3$  (16) or on silica (31); the intermediate species observed from isobutene on HZSM5 should not be due, therefore, to alkoxy groups on extraframework alumina or on nonacidic silanols. Accordingly, under the conditions of the experiment of Fig. 7a, the HZSM5 OH band at  $3745\text{ cm}^{-1}$ , due to nonacidic silanols, is found to be almost unperturbed. On the other hand, the bands at  $2980$ ,  $1480$ , and  $1405\text{ cm}^{-1}$ , cited above, disappeared when the polymer was formed. We propose that the *tert*-butoxy species is actually the intermediate in the polymer formation. We consequently propose that this *tert*-butyl species is formed on the acidic OHs of the zeolite as a result of the evolution of the hydrogen-bonded isobutene species, through a proton transfer. This species would have a carbocationic nature, thus playing the role of an initiator of the cationic polymerization reaction (Scheme I). The higher stability of this monomeric carbenium ion, starting from isobutene, is associated with the partially hindered diffusion of the branched olefin isobutene

into the cavities of the zeolite at low temperature. This tends to hinder the polymer formation. In effect, the channel diameters of the HZSM5 10-membered rings are between  $5.1$  and  $5.6\text{ \AA}$ , which just correspond to the critical diameter expected for isobutene (32). Linear butenes are less hindered and diffuse easier on the cavities. Millini and Rossini (9), on the basis of molecular mechanics calculations, showed that the energy barrier for diffusion in MFI-type zeolites is only slightly higher for isobutene than for 1-butene. However, this difference may be relevant near room temperature. At higher temperatures, the isobutene diffusion is easier, and the polymer is formed. According to our experimental results and our interpretation, the



SCHEME I. Proposed structures for the alkoxide and the carbenium ion initiator of isobutene cationic polymerization on ZSM5.



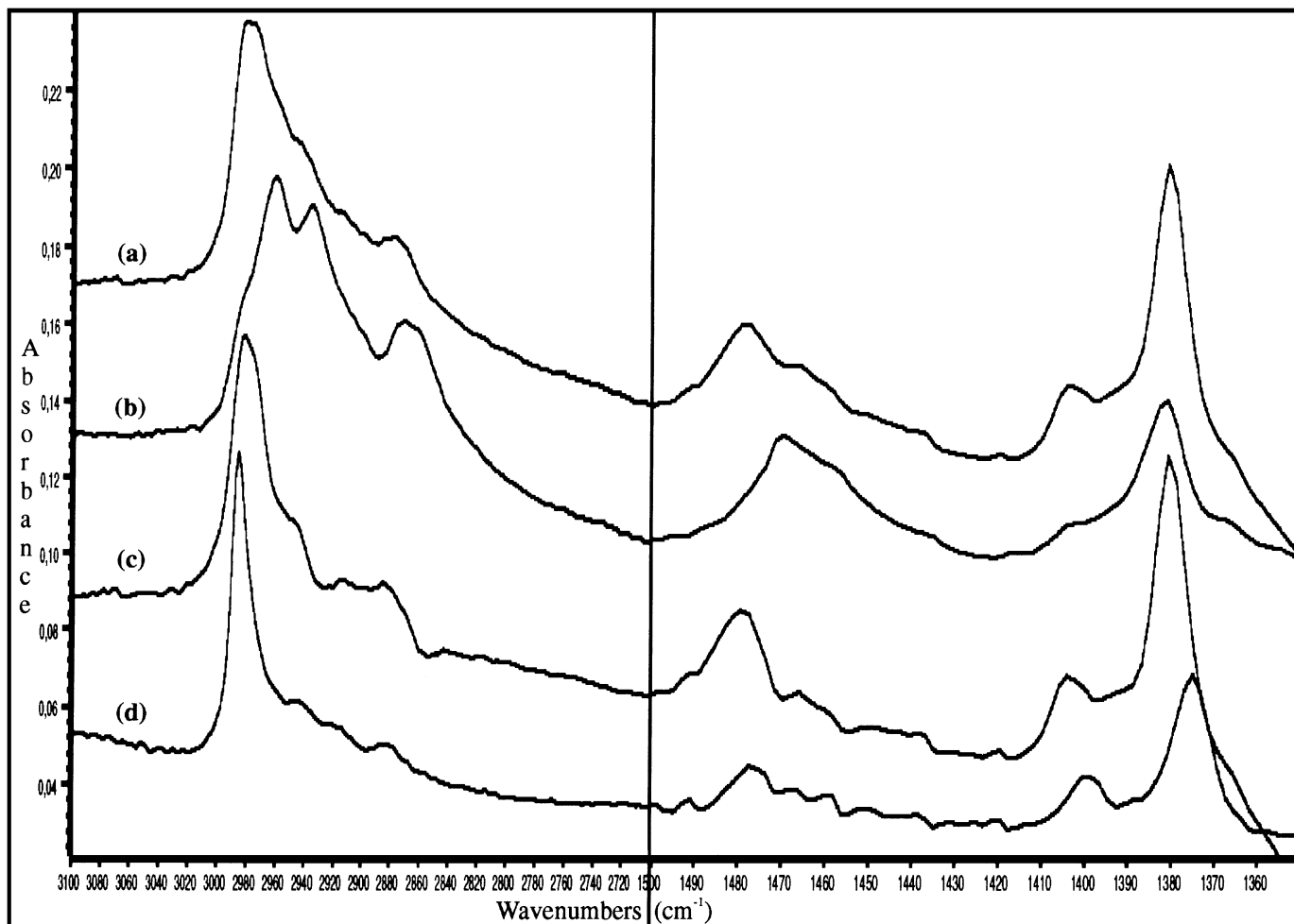
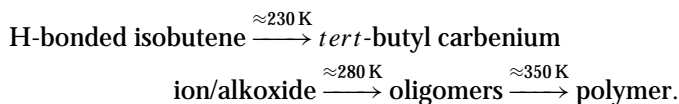


FIG. 7. FT-IR spectra of the adsorbed species arising from (a) isobutene adsorption on HZSM5 at 250 K; (b) isobutene adsorption on HZSM5 at 310 K; (c) subtraction (a)–0.3 (b); (d) *tert*-butanol adsorption on amorphous silica at 373 K outgassing.

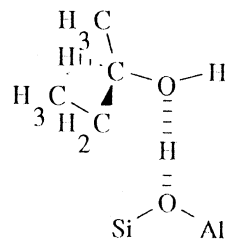
following scheme is proposed as a result of the isobutene interaction:



#### (e) Interaction of 2-Butanol with the HZSM5 Surface

Figure 8 summarizes the results of the experiments on the interaction of 2-butanol on HZSM5. The interaction at room temperature, followed by outgassing, causes the almost complete disappearance of the strongest  $\nu\text{OH}$  band of the zeolite at  $3620 \text{ cm}^{-1}$ , indicating that the strongest Brønsted acid sites are involved in the interaction. On the contrary, the nonacidic silanol groups ( $\nu\text{OH}$  band at  $3746 \text{ cm}^{-1}$ ) are almost unperturbed under these conditions. A strong new  $\nu\text{OH}$  band is found at  $3552 \text{ cm}^{-1}$  and is fairly broad. This band must be assigned to a hydroxy group only weakly perturbed. It seems very feasible to propose an assignment to the OH group of an undissociated alcohol

molecule that interacts through one oxygen lone pair via H-bonding with the strongly acidic zeolite OHs (Scheme II). The  $\nu\text{OH}$  band for monomeric 2-butanol in  $\text{CCl}_4$  solution is observed at  $3627 \text{ cm}^{-1}$ , and a shift down of nearly  $70 \text{ cm}^{-1}$  for H-bonding on the oxygen lone pair seems to be quite reasonable. Similarly, a relatively strong band, slightly split at  $1340, 1315 \text{ cm}^{-1}$ , is associated to the COH deformation of this species upon which the C–H deformation of the



SCHEME II. Proposed structure for the H-bonded 2-butanol/ZSM5 surface complex.

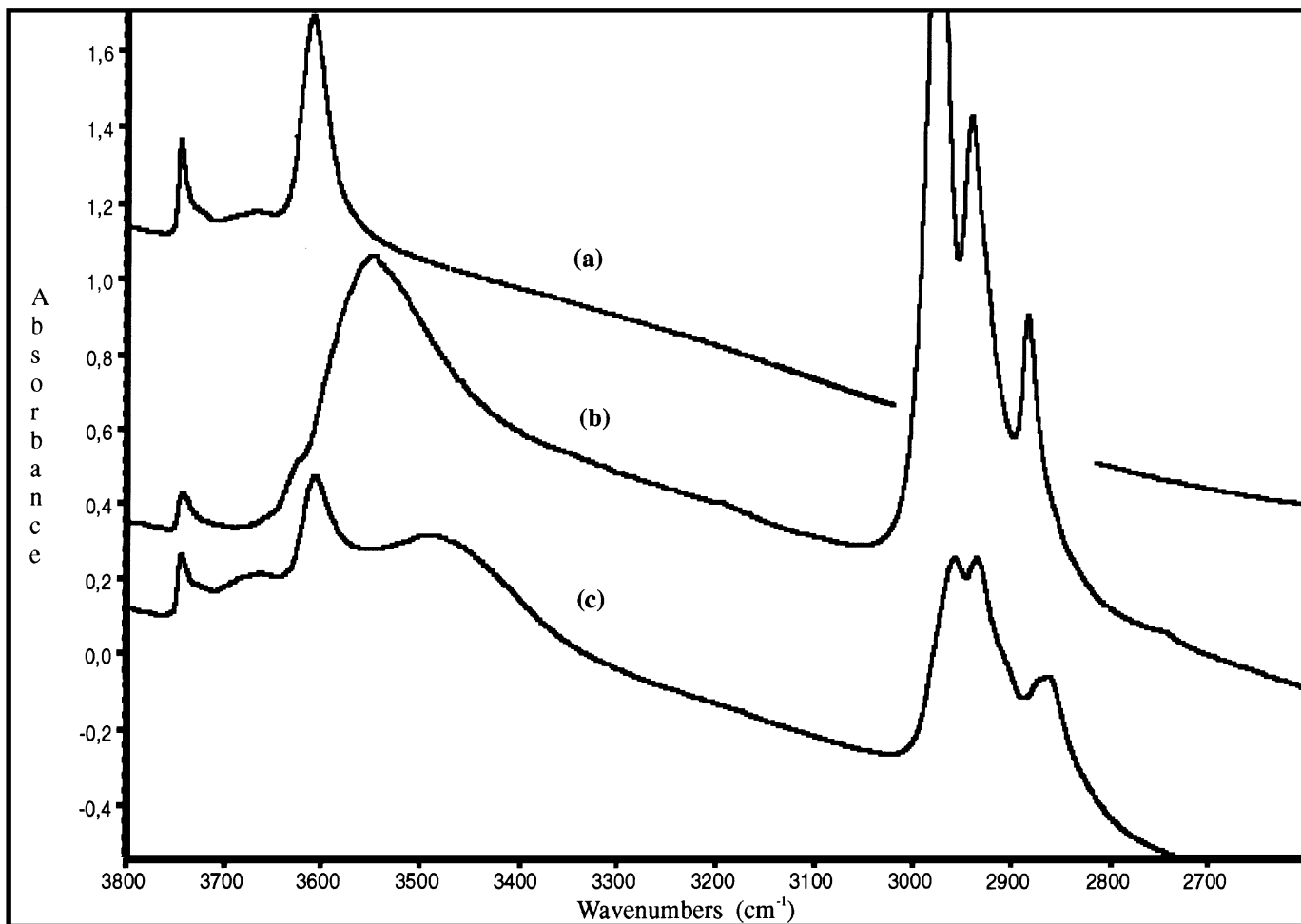


FIG. 8. FT-IR spectra ( $3800\text{--}2600\text{ cm}^{-1}$ ) of the HZSM5 catalyst in the OH/CH stretching region, after outgassing at 773 K (a), after contact with 2-butanol gas, 5 Torr ( $= 666.5\text{ N m}^{-2}$ ), and outgassing at 300 K (b) and 373 K (c).

methine group should be superimposed. We observed the COH and C–H deformations in polymeric liquid 2-butanol at  $1327$  and  $1300\text{ cm}^{-1}$ . Simultaneously, a strong very broad absorption in the region  $2000$  to  $1400\text{ cm}^{-1}$  is observed. This band is mainly associated to the vibrations of the acidic OHs of the zeolite interacting with the oxygen lone pair of 2-butanol, thus providing evidence of a very strong interaction and a partial proton transfer to the alcohol molecule. The  $\text{CH}_3$  and  $\text{CH}_2$  stretching and deformation modes of 2-butanol, observed at  $2976$ ,  $2941$ ,  $2884$ ,  $1465$ ,  $1458$ ,  $1440$  (weak shoulder), and  $1387\text{ cm}^{-1}$ , are only weakly shifted with respect to the liquid alcohol, although with important intensity modifications.

H-bonding interactions of several different bases with different acidic zeolites were investigated recently by Zecchina *et al.* (33). These authors showed that strong H-bonding interactions gave rise to the very broad absorptions extending to the entire near-IR range with the so-called A, B, C contours. This is due to the Fermi resonance of the  $\nu\text{OH}$  mode (very perturbed and shifted down) with

the first overtones of the corresponding in-plane ( $\delta\text{OH}$ ) and out-of-plane ( $\gamma\text{OH}$ ) deformations. When the proton affinity of the adsorbed base is sufficiently high, the C component, typically centered in the region  $2000\text{--}1300\text{ cm}^{-1}$ , becomes predominant.

Outgassing at 373 K strongly modified the picture. All the above features disappeared, while a moderately strong spectrum was still detected, similar to that observed after the interaction of all C4 olefins at room or slightly higher temperatures, assigned above to polyisobutene. This result is interpreted as evidence of the Brønsted acid-induced dehydration of the alcohol to *n*-butene and the subsequent polymerization/isomerization to give the branched polymer.

Similar experiments using *tert*-butanol gave similar results. The H-bonded alcohol is predominant at room temperature while polyisobutene, already present at room temperature, is predominant at 373 K. Production of oligomeric species from C4 alcohols on NaHZSM5 zeolite has already been reported (34).

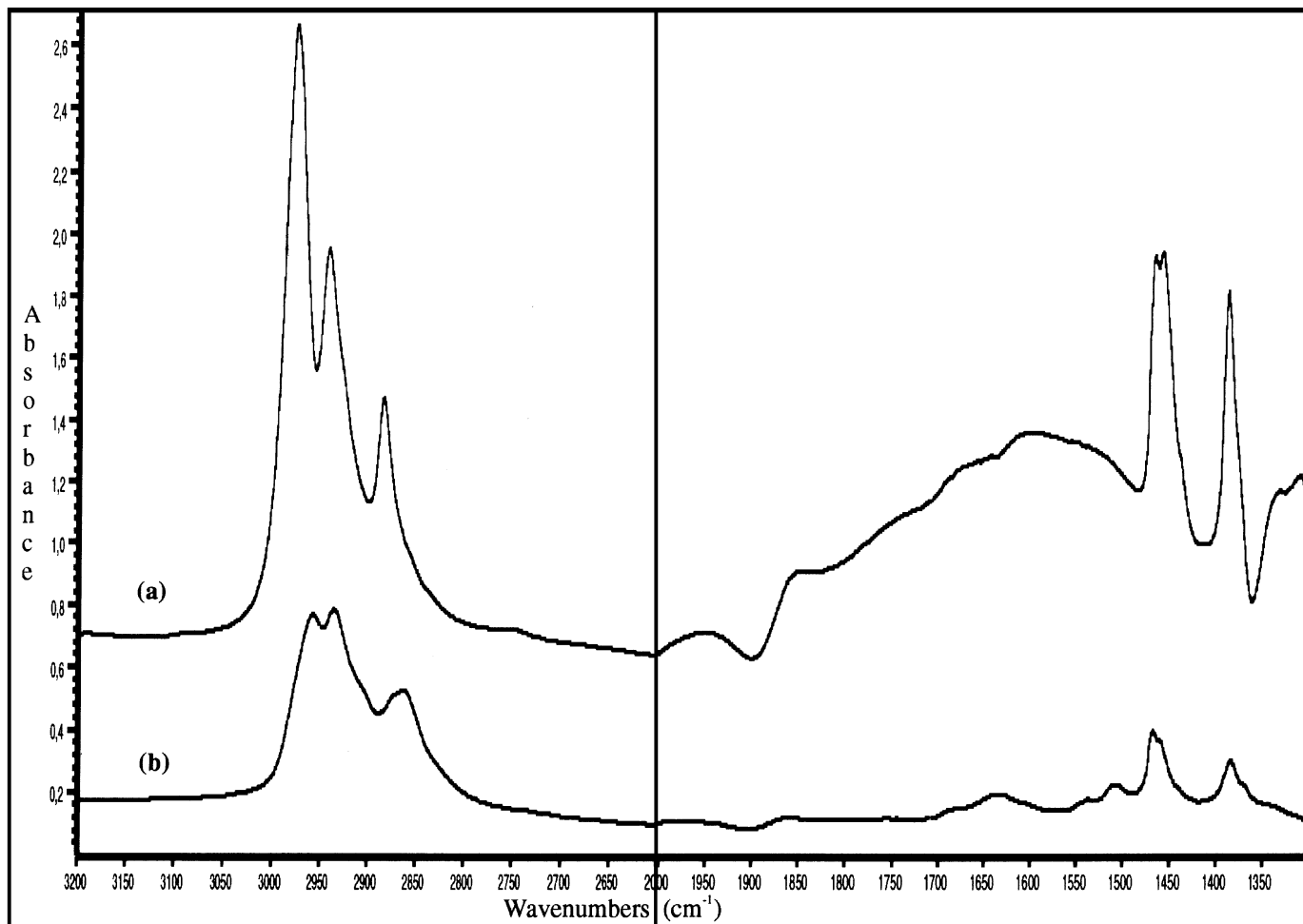


FIG. 9. FT-IR spectra of the adsorbed species arising from 2-butanol adsorption on HZSM5, 5 Torr ( $= 666.5 \text{ N m}^{-2}$ ), and outgassing at 300 K (a) and 373 K (b).

## DISCUSSION

The above results give an indication of the behavior of C4 compounds in contact with very strong protonic acid solids such as HZSM5 zeolite. We observed several interactions:

1. H-bonding of the acidic OHs with the olefinic C=C  $\pi$  orbitals, evident at temperatures below 260 to 290 K for *n*-butenes and below 230 K for isobutene.

2. In the case of isobutene, proton transfer giving rise to an intermediate species, identified as a *tert*-butoxy species formed on the acidic zeolite OHs at 230 to 270 K. This species apparently acts as the initiator of cationic oligomerization that becomes fast near room temperature.

3. Proton-induced cationic isomerization/polymerization of *n*-butenes to give polyisobutene, evident in the range 260 to 290 K.

4. Strong H-bonding of the acidic OHs with the 2-butanol oxygen lone pair evident near room temperature.

5. Proton-induced dehydration/isomerization/polymerization of 2-butanol giving rise to polyisobutene at 300 to 370 K.

6. Proton-induced dehydration/polymerization of *tert*-butanol, already active near 300 K.

7. Depolymerization of polyisobutene and restoring of the acidic surface hydroxy groups of the zeolite at 473 to 573 K.

These data, including the evident higher reactivity of the branched compounds (isobutene and *tert*-butanol) with respect to the linear ones (*n*-butene and 2-butanol), strongly support the hypothesis that carbenium ions are involved. We clearly detected the previous step of carbenium ion formation at low temperature in all butene isomers (i.e., hydrogen bonding) and further steps (oligomerization).

Only in the case of isobutene did we directly detect an intermediate species which is more closely related to a carbenium ion and which we identified as a *tert*-butoxy species. We previously proposed that alkoxy groups on

acidic surfaces can be taken as “equivalent” to carbenium ions (35). Similarly, by theoretically studying the protolytic dehydrogenation of isobutane on protonic zeolites, Kazansky *et al.* (36) recently proposed that a surface *tert*-butoxide intermediate is formed as an intermediate. According to these authors, these alkoxy groups are “the precursors of adsorbed carbenium ions.” In the present case, we detected similar intermediates only from isobutene, very likely due to isobutene diffusion that limits the availability of isobutene, thus allowing the alkoxide “polymer initiator” species to gain sufficient lifetime to be detected.

On the other hand, polyolefins can be produced by cationic polymerization on HZSM5 (8). The formation of polymeric species from olefins on several Brønsted acid solids at room temperature has already been reported (37) and was described in detail using IR spectroscopy for the ethylene/HZSM5 (38, 39) and for the propene/HZSM5 (39–41) systems. In the case of ethylene and propylene interaction with HZSM5, Spoto *et al.* (39) also described the features of the hydrogen-bonded species, assumed to be the precursors of polymerization. We described similar complexes on the OHs of silica (42) and alumina (16). The most significant features of these species are summarized in Table 2. It is evident that the interaction strength of the olefins with the OHs of these materials follows the trend silica < alumina < HZSM5 and the trend ethylene < propylene < *n*-butenes < isobutene. These trends are deduced from the extent of perturbation both of the OH stretching bands of the surface OHs of the catalyst and of the C=C stretching of the olefins; they are related to the increasing interaction strength with increasing Brønsted acidity of the surface OHs of the catalyst and with increasing electron densities at the olefinic double bonds. Thus the interaction of the strongly acidic OHs of HZSM5 and the electron-rich olefin isobutene allows proton transfer to occur easily and allows us to detect the alkoxy species precursor for the carbenium ion transition state at low temperature.

These IR data agree nicely with those arising from <sup>13</sup>C NMR studies, which also allowed the characterization

of oligomeric species formed by the interaction of ethylene (43, 44), propylene (43, 45), and isobutene (43) over HZSM5.

In the present case, an additional question arises concerning the formation of polyisobutene from *n*-butenes, denoted above as isomerization/polymerization. This complex process can occur with different reaction sequences. The simplest are the following.

(a) Protonation of *n*-butenes to *sec*-butyl cation; skeletal isomerization of the *sec*-butyl cation to *tert*-butyl cation; proton elimination to form isobutene; proton-induced cationic polymerization of isobutene. This is an isomerization-followed-by-polymerization way.

(b) Protonation of *n*-butenes to *sec*-butyl cation; skeletal isomerization of *sec*-butyl cation to *tert*-butyl cation; electrophilic attack on an *n*-butene monomer to give a dimer; skeletal isomerization of the dimeric carbenium ion to give an isobutene dimeric carbenium ion; second attack on an *n*-butene monomer to give a trimeric carbenium ion; skeletal isomerization of the trimeric carbenium ion to give an isobutene trimeric carbenium ion; and so on. This can be denoted as an isomerization–polymerization–isomerization way.

(c) Protonation of *n*-butenes to *sec*-butyl cation; electrophilic attack on an *n*-butene monomer to give a dimer; skeletal isomerization of the dimeric carbenium ion to give a branched dimeric carbenium ion; electrophilic attack on an *n*-butene monomer to give a trimer; skeletal isomerization of the dimeric carbenium ion to give a branched trimeric carbenium ion; and so on. This can be denoted as a polymerization-followed-by-isomerization way.

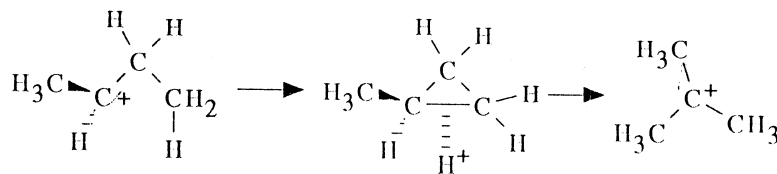
The first sequence implies that skeletal isomerization of the monomeric olefins already occurs at 260–290 K before oligomerization. However, if this were correct, then we should expect to detect isobutene after adsorption of *n*-butenes. Instead, we have no evidence of “free” isobutene interaction with *n*-butenes but observe only its polymer. Thus that we have no support of mechanism (a). Indeed, our data are more in favor of mechanism (b) or (c), but

TABLE 2  
Spectroscopic Data on H-Bonded Olefin Complexes on Hydroxylated Catalyst Surfaces

Catalyst	Shift <sup>a</sup>	Ethylene	Propylene	1-Butene	<i>cis</i> -2-Butene	<i>trans</i> -2-Butene	Isobutene
am SiO <sub>2</sub>	ΔνOH	115	155	155	195	195	220
	ΔνC=C	7	13	8	13	14	10
γ-Al <sub>2</sub> O <sub>3</sub>	νOH	—	3517	3529	3480	3498	3457
	ΔνOH <sup>b</sup>	—	150–250	200–300	200–300	200–300	200–300
	ΔνC=C	—	16	11	16	20	17
HZSM5	ΔνOH	390	540	600	600	600	600
	ΔνC=C	11	19	17	22	27	21

<sup>a</sup> cm<sup>-1</sup>.

<sup>b</sup> A range is given because several different OH groups exist and all shift down.



SCHEME III. Mechanism of *sec*-butyl to *tert*-butyl carbenium ion transposition via protonated alkylcyclopropane.

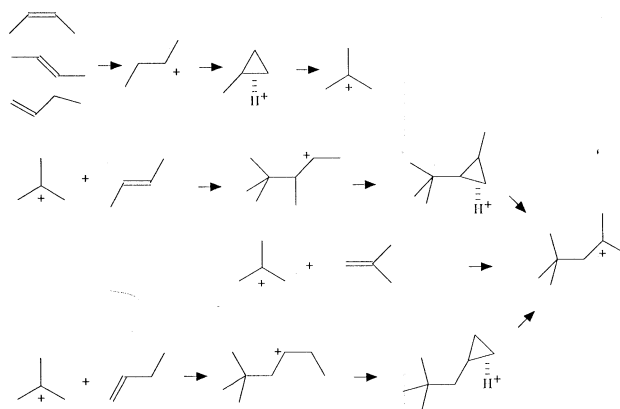
we cannot easily discriminate between them on the basis of the present experimental results. These two mechanisms differ in relation to the fact that mechanism (b) forecasts the skeletal isomerization of both monomeric and polymeric secondary carbenium ions, while mechanism (c) consists at the skeletal isomerization of polymeric carbenium ions only.

The discrimination between mechanisms (b) and (c) may be related to the current discussion on the mechanism of *n*-butene skeletal isomerization. According to Mooiveer *et al.* (3) and to Guisnet *et al.* (46), both working on ferrierite, the predominant mechanism is "bimolecular" and goes through C8 dimeric species. However, according to Asensi *et al.* (7), working on MCM22, and to Millini and Rossini (9), working on different zeolites, the predominant mechanism should be monomolecular.

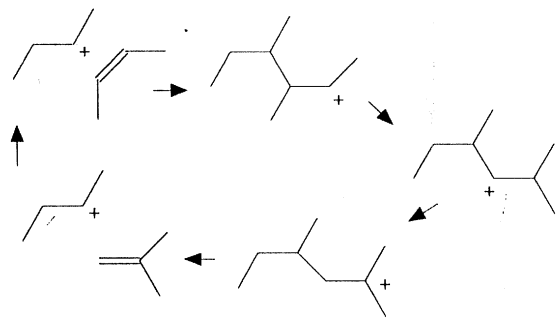
Literature data indicate that skeletal isomerization of the *sec*-butyl carbenium ion is definitely slower than that of *n*-pentyl or higher carbenium ions (13, 14). According to some authors (3, 13, 46), this is due to the fact that the isomerization of the *sec*-butyl cation necessarily goes through the unfavorable formation of the primary isobutyl carbenium ion. However, according to Brouwer and Hogeveen (13), the *sec*-butyl to *tert*-butyl isomerization can occur through the formation of protonated methylcyclopropane (Scheme III), whose ring opening to give the *tert*-butyl cation could be concerted. This avoids the formation of the primary isobutyl carbenium ion. This is deduced by these authors (13) from the activation energy of this process, higher than for C5 carbenium ion isomerization but too low to allow the intermediacy of a primary carbenium ion. Another possibility (3) is that the C4 carbenium ion skeletal isomerization goes through a previous dimerization to a C8 carbenium ion, which can isomerize without going through a primary carbenium ion, and later crack to iso-C4 species (14). On the other hand, Guisnet *et al.* (46) recently showed that the dimerization of the *sec*-butyl cation on ferrierite is a slow step, much slower than the skeletal isomerization of a C8 dimeric carbocation. Moreover, the determination of the effect of process variables on reaction selectivities (which could show whether C8 is indeed an intermediate in the reaction) requires more sophisticated analytical procedures than those used by most researchers. Finally, the observed trends of product selectivities allowed Asensi *et al.* (7) to exclude the "bimolecular" mechanism as being predominant on MCM22.

Interestingly, the spectrum of the polymer, which we observed to be formed from all four C4 olefins (Fig. 4) and from C4 alcohols, is virtually identical to that reported by Spoto *et al.* (39), who found that it was formed from ethylene on HZSM5 at room temperature and short contact times. Spoto *et al.* (39) showed that the typical spectrum of polyethylene develops from ethylene on HZSM5 only after relatively high contact times (more than 130 s). The authors of Ref. (39) recognized that, after very short contact times with ethylene gas, the absorption bands of methyl groups are certainly present but, with a rough evaluation of the relative intensities of the bands, they assigned the spectrum to a dimeric or a trimeric alkyl species, i.e., to *n*-butyl or *n*-hexyl species. The identity of the spectrum that they reported (and we confirmed experimentally) to arise from ethylene combined with what we report here for isobutene oligomerization definitely supports the idea that the *n*-butyl species formed by ethylene cationic dimerization undergoes at room temperature skeletal isomerization to *tert*-butyl species, just as occurs for *sec*-butyl species arising from *n*-butene protonation. This is quite obvious and should occur through the formation of the same protonated methylcyclopropane intermediate.

These data strongly support the proposal that, on HZSM5 cavities at temperatures as low as 270 K, skeletal isomerization of the linear C4 carbenium ions, arising from both C2 and C4 olefins, occurs, thus giving rise to the most stable species, the *tert*-butyl carbenium ions. Mechanism (b), reported in Scheme IV, therefore seems to be the best



SCHEME IV. Proposed mechanism for the production of polyisobutene from *n*-butenes and from isobutene with the intermediacy of protonated cyclopropane carbenium ions.



SCHEME V. A possible mechanism for *n*-butene skeletal isomerization via isomerization of dimeric carbenium ions as proposed in Ref. (3).

one to rationalize our experimental results, and, indirectly, also those of Spoto *et al.* (39). Consequently, the behavior we observed supports the proposal that monomeric linear C4 carbenium ions can isomerize on HZSM5 cavities at very low temperatures. Thus the "classical" monomolecular skeletal isomerization mechanism for butenes via protonated methylcyclopropane (11, 13) is also supported.

The isobutene polymer, produced at very low temperature from C4 olefins and alcohols, tends to depolymerize (and possibly to partly crack) at 473 to 573 K according to thermodynamics and to our experimental results. The formation of the same oligomeric species from C<sub>4</sub> and C<sub>2</sub> compounds and their cracking can be related to the formation of nearly the same hydrocarbon mixtures from any hydrocarbon reactant on HZSM5, as reported by Chen and colleagues (8). The decomposition temperature of polyisobutene species is slightly higher than that reported for the production of oligomers of propene on HZSM5 at 35 atm (473 K (8)). This means that, even though at the temperatures of an industrial process for butene isomerization, namely 620 to 720 K, the carbenium ion transposition is a very fast process on HZSM5, the reaction temperature cannot be decreased very much just to avoid formation of oligomeric species. This makes the very high activity of the protonic centers of ZSM5 zeolite partly unuseful or even noxious. In fact, in the temperature range where the reaction must be carried out in order to limit oligomerization, this material is already very active in side reactions like cracking and coking.

On the other hand, "clean" protonic zeolites, such as HZSM5, are not very selective catalysts for *n*-butene skeletal isomerization, but some of them (e.g., ferrierite (47)) become more selective catalysts after partial coking. This effect could result from the deactivation of the most active acidic OH groups, very active in cracking. This explains why much weaker Brønsted solid acids (e.g., pure alumina and silicated alumina), by far cheaper and more stable in regeneration cycles than most zeolites, can compete and act as even better catalysts at such high temperatures than those necessarily applied in an industrial *n*-butene skeletal isomerization process.

## CONCLUSIONS

The main conclusions from the present study can be summarized as follows:

1. HZSM5 zeolite is very active in converting *n*-butenes at 733 K, but the selectivity to isobutene is low. Cracking products, C<sub>4</sub> paraffins, and aromatics are the main by-products.
2. IR studies show that *n*-C<sub>4</sub> olefins undergo isomerization/polymerization sequences to give polyisobutene in all cases at 260 to 290 K.
3. Isobutene gives rise to polyisobutene species at 230 to 270 K.
4. *tert*-Butoxy species are found to act as intermediates in isobutene cationic polymerization.
5. The same polymeric species are also formed from *sec*-butanol and *tert*-butanol, though at higher temperatures (300–370 K).
6. Polyisobutene species depolymerize at 473 to 573 K.
7. These data are interpreted as a support to the monomolecular mechanism for *n*-butene skeletal isomerization to isobutene.

## REFERENCES

1. Butler, A. C., and Nicolaides, C. P., *Catal. Today* **18**, 443 (1993).
2. U.S. Clean Air Act Amendments (Public Law 101-549, November 15, 1990).
3. Grandvallet, P., DeJong, K. P., Mooiweer, H. H., Kortbeek, A. G. T. G., and Kraushaar-Czarnetzki, B., EP Patent 501577 (1992); Mooiweer, H. H., DeJong, K. P., Kraushaar-Czarnetzki, B., and Stork, W. H. J., *Stud. Surf. Sci. Catal.* **84**, 2327 (1994).
4. Simon, M. W., Suib, S. L., and O'Young, C. L., *J. Catal.* **147**, 484 (1994).
5. Xu, W. Q., Yin, Y. G., Suib, S. L., and O'Young, C. L., *J. Catal.* **150**, 34 (1994); O'Young, C. L., Pellet, R. J., Casey, D. G., Ugolini, J. R., and Sawicki, R. A., *J. Catal.* **151**, 467 (1995).
6. Pellet, R. J., Casey, D. G., Huang, H. M., Kessler, R. V., Kuhlman, E. J., O'Young, C. L., Sawicki, R. A., and Ugolini, J. R., *J. Catal.* **157**, 423 (1995).
7. Asensi, M. A., Corma, A., and Martinez, A., *J. Catal.* **158**, 561 (1996).
8. Chen, N. Y., "Shape Selective Catalysis in Industrial Applications," p. 67. Dekker, New York, 1989.
9. Millini, R., and Rossini, S., "Proceedings, 11th Int. Conference on Zeolites, Seoul, Korea, 1996," in "Studies Surface Science and Catalysis," Vol. 105 B, p. 1389. Elsevier, Amsterdam, 1997.
10. Wojciechowski, B. W., and Corma, A., "Catalytic Cracking," Dekker, New York.
11. Gates, B. C., "Catalytic Chemistry," Wiley, New York, 1992.
12. Olah, G. A., and Molnar, A., "Hydrocarbon Chemistry," Wiley, New York, 1995.
13. Brouwer, D. M., and Hogeveen, H., *Prog. Phys. Org. Chem.* **9**, 179 (1972).
14. Brouwer, D. M., in "Chemistry and Chemical Processes" (R. Prins and G. C. A. Schuit, Eds.), p. 137. Sythoff and Noordhoff, Groningen, 1980.
15. Finocchio, E., Busca, G., Rossini, S. A., Cornaro, U., Piccoli, V., and Miglio, R., *Catal. Today* **33**, 335 (1997).
16. Trombetta, M., Busca, G., Rossini, S. A., Piccoli, V., and Cornaro, U., *J. Catal.* **168**, 334 (1997).

17. Buonomo, F., Fattore, V., and Notari, B., U.S. Patent 4013589 (1977); Buonomo, F., Fattore, V., and Notari, B., U.S. Patent 4013590 (1977); Manara, G., Fattore, V., and Notari, B., U.S. Patent 4038337 (1977).
18. Kilpatrick, J. E., Prosen, E. J., Pitzer, K. S., and Rossini, F. D., *J. Res. Natl. Bur. Stand.* **36**, 559 (1946).
19. Quin, G., Zheng, L., Xie, Y., and Wu, C., *J. Catal.* **95**, 609 (1985).
20. Kustov, L. M., Kazansky, V. B., Beran, S., Kubelkova, L., and Jiru, P., *J. Phys. Chem.* **91**, 5247 (1987).
21. Zecchina, A., Bordiga, S., Spoto, G., Scarano, D., Petrini, G., Leofanti, G., Padovan, M., and Otero Arean, C., *J. Chem. Soc. Faraday Trans.* **88**, 2959 (1992).
22. Astorino, E., Peri, J. B., Willey, R. J., and Busca, G., *J. Catal.* **157**, 482 (1995).
23. Lin-Vien, D., Colthup, N. B., Fateley, W. G., and Grasselli, J. G., "The Handbook of Infrared and Raman Characteristic Frequencies of Organic Molecules." Academic Press, San Diego, 1991.
24. Goldbach, G., and Peitscher, G., *J. Polym. Sci. Part B* **6**, 783 (1968).
25. Bowling Barnes, R., Liddel, U., and Williams, Z., *Ind. Eng. Chem.* **15**, 659 (1943).
26. Pouchert, C. J., "The Aldrich Library of FT-IR Spectra," Vol. 1, p. 1162 B. Aldrich Chemical, Milwaukee, WI, 1985.
27. Kozyreva, M. S., *Opt. Spectrosc.* **6**, 303 (1959).
28. Demidov, A. V., and Davydov, A. A., *Mater. Chem. Phys.* **39**, 13 (1994).
29. Lide, D. R. (Ed.), "Handbook of Chemistry and Physics," 72nd ed., CRC Press, Boca Raton, FL, 1991.
30. Ramis, G., Busca, G., and Lorenzelli, V., *J. Chem. Soc. Faraday Trans. I* **83**, 1591 (1987).
31. Busca, G., Ramis, G., and Lorenzelli, V., *J. Chem. Soc. Faraday Trans. I* **85**, 137 (1989).
32. Bhatia, S., "Zeolites Catalysis: Principles and Applications." CRC Press, Boca Raton, FL, 1989.
33. Zecchina, A., Buzzoni, R., Bordiga, S., Geobaldo, F., Scarano, D., Ricchiardi, G., and Spoto, G., in "Zeolites, a Refined Tool for Designing Catalytic Sites" (T. Bonneviot and S. Kaliaguine, Eds.), p. 213. Elsevier, Amsterdam, 1995; Zecchina, A., paper presented at the "Discussions in Catalytic Chemistry—Catalysis by Strong Solid Acids, Baltimore, July 6–7, 1996"; Zecchina, A., Bordiga, S., Spoto, G., Scarano, D., Spanò, G., and Geobaldo, F., *J. Chem. Soc. Faraday Trans.* **92**, 4863 (1996).
34. Williams, C., Makarova, M. A., Malysheva, L. V., Paukshtis, E. A., Zamaraev, K. I., and Thomas, J. M., *J. Chem. Soc. Faraday Trans. I* **86**, 3473 (1990).
35. Busca, G., Finocchio, E., Ramis, G., and Ricchiardi, G., *Catal. Today* **32**, 133 (1996).
36. Kazansky, V. B., Frash, M. V., and vanSanten, R. A., in "11th Int. Congr. on Catalysis—40th Anniversary" (J. W. Hightower, W. N. Delgass, E. Iglesia, and A. T. Bell, Eds.), p. 1233. Elsevier, Amsterdam, 1996.
37. Busca, G., Lorenzelli, V., Ramis, G., and Sanchez Escribano, V., *Mater. Chem. Phys.* **29**, 175 (1991).
38. Bolis, V., Vadrine, J. C., Vande Berg, J. P., Wolthuizen, J. P., and Derouane, E. G., *J. Chem. Soc. Faraday Trans. I* **76**, 1606 (1980).
39. Spoto, G., Bordiga, S., Ricchiardi, G., Scarano, D., Zecchina, A., and Borello, E., *J. Chem. Soc. Faraday Trans.* **90**, 2827 (1994).
40. McGrady, M. C., and Gorte, R. J., *J. Phys. Chem.* **89**, 1305 (1985).
41. Kiricsi, I., and Förster, H., *J. Chem. Soc. Faraday Trans. I* **84**, 491 (1988).
42. Busca, G., Ramis, G., Lorenzelli, V., Janin, A., and Lavalley, J. C., *Spectrochim. Acta A* **43**, 489 (1987).
43. Van den Berg, J. P., Wolthuizen, J. P., Clague, A. D. H., Hays, G. R., Huis, R., and Van Hooff, J. H. C., *J. Catal.* **80**, 130 (1983); Van den Berg, J. P., Wolthuizen, J. P., and Van Hooff, J. H. C., *J. Catal.* **80**, 139 (1983).
44. Derouane, E. G., Gilson, J. P., and Nagy, J. B., *J. Mol. Catal.* **10**, 331 (1981).
45. Galya, L. G., Occelli, M. L., Hsu, J. T., and Young, D. C., *J. Mol. Catal.* **32**, 391 (1985).
46. Guisnet, M., Andy, P., Gnep, N. S., Benazzi, E., and Travers, C., *J. Catal.* **158**, 551 (1996).
47. Guisnet, M., Andy, P., Gnep, N. S., Travers, C., and Benazzi, E., *J. Chem. Soc. Chem. Commun.*, 1685 (1995).